

# Multi-Modular MANTA-RAY: A Modular Soft Surface Platform for Distributed Multi-Object Manipulation

Pratik Ingle, Jørn Lambertsen, Kasper Støy, Andres Faiña

IT University, Denmark  
 {prin, jrnl, ksty, anfv}@itu.dk

**Abstract**—Manipulation surfaces control objects by actively deforming their shape rather than directly grasping them. While dense actuator arrays can generate complex deformations, they also introduce high degrees of freedom (DOF), increasing system complexity and limiting scalability. The MANTA-RAY (Manipulation with Adaptive Non-rigid Textile Actuation with Reduced Actuation densitY) platform addresses these challenges by leveraging a soft, fabric-based surface with reduced actuator density to manipulate fragile and heterogeneous objects. Previous studies focused on single-module implementations supported by four actuators, whereas the feasibility and benefits of a scalable, multi-module configuration remain unexplored. In this work, we present a distributed modular and scalable variant of the MANTA-RAY platform that maintains manipulation performance with a reduced actuator density. The proposed multi-module MANTA-RAY platform and control strategy employs a object passing between modules and geometric transformation-driven PID controller that directly maps tilt-angle control outputs to actuator commands, eliminating the need for extensive data-driven or black-box training. We evaluate system performance in simulation across surface configurations of varying modules ( $3 \times 3$ , and  $4 \times 4$ ) and validate its feasibility through experiments on a physical  $2 \times 2$  hardware prototype. The system successfully manipulates objects with diverse geometries, masses, and textures—including fragile items such as eggs and apples as well enabling parallel manipulation. The results demonstrate that the muti-module MANTA-RAY improves scalability and enables coordinated manipulation of multiple objects across larger areas, highlighting its potential for practical, real-world applications.

**Index Terms**—Manipulation, Soft Robot, Robotic Manipulation Surface, Distributed

## I. INTRODUCTION

Objects in real-world environments exhibit wide variations in shape, size, and material properties, making it difficult for robotic manipulators to handle them. Conventional grippers, though precise for structured tasks, often fail with irregular or fragile items—too little force leads to slipping, while too much can cause damage. These limitations highlight the need for adaptable, contact-rich manipulation strategies that can generalize across diverse object types.

In recent years Robotic Manipulation Surfaces (RMS) have emerged as a promising approach to address these challenges. Rather than grasping objects directly, RMS platforms manipulate them by dynamically deforming or actuating the surface on which the objects rest. Arrays of actuators generate local deformations or motions that leverage friction, gravity, and vibration to reposition one or multiple objects simultaneously. The distributed contact area provided by such surfaces allows safe and coordinated manipulation,

particularly advantageous for fragile or large, flat objects that benefit from uniform support.

Several RMS designs been proposed over the time. Wheel-based systems [1], [2] use omnidirectional rollers to transport items efficiently but struggle with small or uneven objects that cannot maintain stable contact. Piston-based arrays [3], [4] offer precise local control by vertically actuating dense grids of pins, enabling translation and rotation. However, their reliance on high actuator density increases mechanical complexity, cost, and control overhead. Other approaches—such as vibrating plates [5], [6], air-flow levitation [7], cilia-inspired actuators [8], and deformable gel layers [9]—demonstrate unique advantages but remain limited by trade-offs in payload, versatility, or scalability.

To address these challenges, Chih-Han et al. [10] proposed *Morpho*, a self-deformable modular robot inspired by cellular structures that enables large-scale shape morphing for diverse global functions. Using neoprene and latex membranes, it demonstrates potential for surface-based object manipulation but focuses primarily on inter-module ball transfer rather than precise manipulation. Recently Ingle et al. proposed MANTA-RAY: Manipulation with Adaptive Non-rigid Textile Actuation with Reduced Actuation densitY [11]. A novel system that drastically reduces the hardware and control complexity. It achieves heterogeneous and fragile object manipulation over a large area with only a few actuators. It uses a flexible fabric sheet attached to a small number of linear actuators forming a reconfigurable surface that can tilt and deform in order to move objects indirectly. By interconnecting the actuators with a continuous soft layer, the MANTA-RAY effectively uses the surface itself as a medium to transmit forces to the object, enabling even small or irregular items to be manipulated without falling through gaps. This approach dramatically lowers the actuator count and degrees of freedom [12] compared to traditional RMS. The reduced hardware not only cuts down on system cost and weight, but also simplifies control since there are far fewer motors to coordinate. Even with fewer actuators, MANTA-RAY preserves versatile manipulation performance [13], as its compliant fabric surface conforms to object geometry and safely handles fragile items—including eggs and fruits—without damage. Notably, the system achieves an object-to-actuator size ratio as low as 0.01 (i.e., objects can be  $100 \times$  smaller than the spacing between actuators) – far beyond what previous manipulation surfaces could achieve.

Despite its advantages, heterogeneous object manipulation

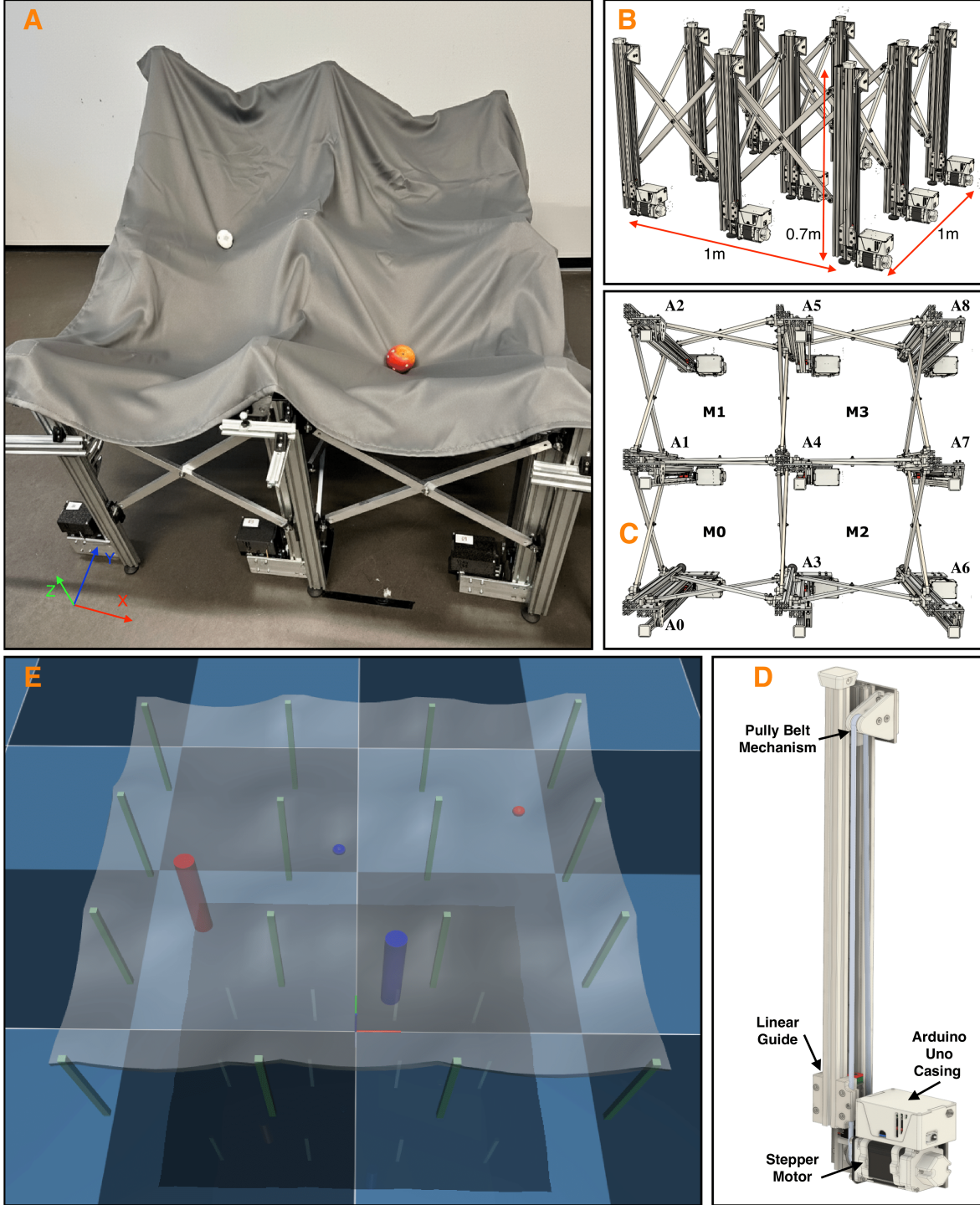


Fig. 1: **Multi-Modular MANTA-RAY**: Manipulation with Adaptive Non-rigid Textile Actuation with Reduced Actuation density platform. (A) Manipulation of an egg and an apple. (B) Side view showing the platform dimensions of  $1 \times 1 \times 0.7$  m (length, width, and height at rest). (C) Top view illustrating the arrangement of nine actuators (A0–A8) and four modules (M0–M3) without the flexible surface. (D) Each linear actuator has 0.4-meter vertical range and built using a stepper motor and pulley-belt mechanism, controlled by an *Arduino Uno* micro controller. (E) MuJoCo simulation of the extended 3  $\times$  3-module configuration showing two objects (red and blue spheres) and their respective target locations.

has so far been demonstrated only on a single MANTA-RAY module, where the surface is supported and controlled by exactly four actuators. The potential benefits and feasibility of extending this design into a multi-modular configuration—where multiple actuators are arranged in a grid to form several independent modules, each supported by four actuators—remain largely unexplored. This limitation primarily arises from the absence of an effective multi-module control framework and compatible hardware design. A multi-modular MANTA-RAY architecture, however, introduces the possibility of *parallel manipulation*, enabling the simultaneous handling of multiple heterogeneous objects across interconnected modules.

In this work, we propose a multi-modular, distributed MANTA-RAY platform capable of manipulating heterogeneous objects and achieving parallel, coordinated manipulation across multiple modules. In the hardware implementation, each actuator functions as an independent unit, enhancing the system’s robustness to individual actuator faults. The modular design further allows adjustable actuator spacing to accommodate various workspace dimensions and application requirements. We demonstrate that a classical linear controller, integrated with an object-passing strategy, can effectively control this inherently soft and non-linear system when combined with an appropriate geometric transformation. This approach enables seamless object transfer between neighboring modules, allowing continuous, robust, and efficient manipulation across the entire surface.

## II. MULTI-MODULAR MANTA-RAY

The single-module MANTA-RAY platform manipulates objects on a soft fabric surface using four linear actuators placed at the corners of a square and that move vertically and change the slope of the fabric. To extend its scalability, we developed a  $3 \times 3$  actuator grid configuration, forming a  $2 \times 2$  multi-modular MANTA-RAY platform (see Fig.1). Each module (M0–M3) consists of four actuators selected from the nine available actuators (A0–A8), as shown in Fig.1C. Adjacent modules share two actuators; for example, actuators A3 and A4 are shared between Modules M0 and M2. In this multi-modular implementation, the spacing between the actuators can be changed easily by a scissor mechanism making it a reconfigurable platform. For the experiments carried out in this work, the actuators are spaced 0.5 m apart, resulting in an overall platform size of  $1 \times 1$ m and a resting height of 0.7 m. Each actuator provides a vertical stroke of 0.4 m, allowing the surface to generate inclined planes or wave-like deformations. By modulating the relative actuator heights, the system forms controlled gradients that guide object motion across the fabric surface.

Previous work [13] identified three primary mechanisms for object manipulation on soft surfaces: *rolling*, *sliding*, and *pulling*. Rolling occurs when spherical or cylindrical objects move under gravity along an inclined surface, while flat or low-profile objects predominantly slide. Pulling corresponds to indirect motion induced by tension variations within the fabric. In a single MANTA-RAY module, these

motion behaviors are achieved by dynamically deforming the surface through the coordinated actuation of the four linear actuators. The efficiency of manipulation depends on the interplay between object geometry and fabric properties such as friction, elasticity, and surface tension.

The multi-modular MANTA-RAY platform harnesses these same three mechanisms—rolling, sliding, and pulling—scaled across multiple interconnected modules. Rolling and sliding are particularly leveraged to transfer objects between neighboring modules, while each individual module retains the capability to perform independent manipulation. This design enables seamless object transfer and the parallel manipulation of items with diverse shapes, sizes, and weights without direct actuator–object contact.

## III. METHODS

The following sections III-A describe the hardware implementations used for evaluation, III-B present the simulation setup while Sections (III-C) describe the detailed control formulation for Multi-Modular MANTA-RAY.

### A. Hardware Setup:

The  $2 \times 2$  grid modular MANTA-RAY hardware setup consists of 9 linear actuators, connected by a scissor mechanism, making it easier to adjust the distance between the actuators. Each actuator has a 0.4-meter vertical range and is driven by stepper motor (Nema 23 Bipolar model) with  $1.8^\circ$  step angle and 1.85Nm holding torque, which converts rotational motion into linear displacement using a pulley and belt mechanism. The actuators are mounted on a linear guide to ensure smooth and precise movement. A soft manipulation surface, composed of 100% polyester fabric of size  $1.2 \times 1.2$  meter, covers each module with  $0.6 \times 0.6$  meter fabric to facilitate surface hanging. is attached to the actuators and provides a flexible interface for object handling through rolling, sliding, and pulling motions. Each actuator is controlled by an Arduino Uno micro-controller, CNC V3 shield and a A4988 stepper motor driver, which sends PWM signals to motor driver, with real-time position feedback obtained via AS500 magnetic encoders (12-bit resolution). Controller in the Arduino takes desire actuator position and uses a proportional controller to produce the motor speed. Object tracking is achieved using an 6 Optitrack camera system capable of position capturing upto a rate of 200Hz. The modular design allows for adjustments in actuator spacing, fabric properties, and integration of additional modules to scale the system for larger manipulation tasks.

### B. Simulation Setup:

MuJoCo [14] was used as a physics-based simulator to test the controller in a simulation environment. The *flexcomp* and *composite* elements in MuJoCo facilitate the creation of deformable objects, allowing flexible components such as cloth or soft bodies to be defined. The simulation includes three modular platforms: a single-module setup and grids of  $2 \times 2$  and  $3 \times 3$  modules (4 and 9 modules, respectively). Positional actuators with a range of  $[-0.20, 0.20]$  m are

placed at a distance of 0.5 m from each other. A soft fabric is connected on top of the actuator grid to closely mimic the hardware system. The simulation runs at 1000Hz. Figure 1 illustrates the setup.

### C. Controller

The multi-modular MANTA-RAY platform achieves object manipulation through two core control modes: *object passing* for inter-module transfer and *position control* for fine manipulation within an individual module. Both rely on simple geometric deformation principles combined with closed-loop feedback, enabling robust and scalable operation across interconnected modules. The platform controls only the actuators of the module on which the object currently resides, maintaining a low-dimensional (2D) control space and operating efficiently at a control frequency of 20 Hz.

1) *Object Passing*: Objects are transferred between modules using rolling or sliding behaviors, depending on their shape, size, and weight. To induce these behaviors, actuators belonging exclusively to the current module (i.e., not shared with the neighboring module) are raised, while the remaining four actuators—two shared and two belonging to the adjacent module—are lowered. This coordinated actuation creates a temporary local slope that allows the object to roll, slide, or exhibit a combination of both for smooth transfer across module boundaries.

The overall passing process operates hierarchically, as summarized in Algorithm 1. The high-level layer determines the sequence of modules between the current and target positions using a Manhattan-based shortest-path policy, while the low-level layer executes the physical transfer by commanding actuator height adjustments in timed phases. Real-time object tracking via the OptiTrack system provides feedback to confirm successful transfer and trigger adaptive retries if necessary. This two-step strategy enables reliable inter-module transfer of heterogeneous objects while preserving decentralized control across the platform.

In Algorithm 1,  $\mathbf{p}$  and  $\mathbf{p}_d$  denote the current and target object positions, respectively, while  $m_{curr}$  and  $m_{target}$  represent the corresponding source and destination modules. The function `DetectModule()` determines the module containing the object based on its position, and `FindPath()` computes the shortest sequence of intermediate modules using a Manhattan-based path planner. The function `GetActuatorsToRaise()` selects the actuators to be elevated for initiating the object’s movement toward the next module. Parameters  $h_{raise}$  and  $t_{raise}$  define the height and duration of actuator elevation, respectively, while  $t_{settle}$  ensures stabilization after each transfer phase. If object does not pass to next module (line 10 -12) then the the  $h_{raise}$  and  $t_{raise}$  are increased from preferred value. The process iterates until the object successfully reaches the target module, confirmed by position feedback from the tracker.

2) *Position Control*: When both the object and target lie within the same module, a local PID-based controller governs the four actuators supporting the soft surface. Each

---

### Algorithm 1 Object Passing Between Modules

---

**Require:** Object position  $\mathbf{p}$ , target position  $\mathbf{p}_d$ , tracker feedback

**Ensure:** Successful inter-module transfer

```

1:  $m_{curr} \leftarrow \text{DetectModule}(\mathbf{p}), m_{target} \leftarrow \text{DetectModule}(\mathbf{p}_d)$ 
2: while  $m_{curr} \neq m_{target}$  do
3:    $\text{path} \leftarrow \text{FindPath}(m_{curr}, m_{target})$ 
4:    $\text{actuators} \leftarrow \text{GetActuatorsToRaise}(m_{from}, m_{to})$ 
5:   Raise exclusive actuators in  $m_{from}$  opposite to  $m_{to}$ 
6:   Lower shared and neighboring actuators to form slope
7:   Hold for  $t_{raise}$ , then settle for  $t_{settle}$ 
8:   Update  $\mathbf{p}, m_{curr} \leftarrow \text{DetectModule}(\mathbf{p})$ 
9:   if  $m_{curr} \neq m_{to}$  then
10:    Adapt  $h_{raise}$  and  $t_{raise}$  for retry
11:   end if
12: end while
13: return success

```

---

module forms a rectangular workspace of size  $m \times n$  m, providing four degrees of freedom (DOF) for deformation. The controller takes as input the desired target position  $\mathbf{p}_d = (x_d, y_d)$ , the current object position  $\mathbf{p} = (x, y)$ , actuator base coordinates  $\{(x_i, y_i)\}_{i=1}^4$ , and a reference height  $z_0 = 1.5$  m, following the Manhattan controller in [13].

At each control step ( $f = 20$  Hz), positional errors  $e_x, e_y$  are processed by a PID controller to compute surface tilt angles  $\theta_{zx}$  and  $\theta_{zy}$  about the  $X$ - and  $Y$ -axes. The surface orientation is represented by the normal vector

$$\vec{n} = (\sin \theta_{zx}, \sin \theta_{zy}, \cos \theta_{zx}), \quad (1)$$

which defines the plane

$$\vec{n} \cdot (\vec{r} - \vec{r}_0) = 0, \quad \vec{r}_0 = (0, 0, z_0). \quad (2)$$

The desired actuator heights are then derived from the plane geometry as

$$z_i = \frac{z_0 n_z - n_x x_i - n_y y_i}{n_z}, \quad (3)$$

with corresponding actuator commands

$$a_i = (z_0 - z_i) + \alpha \delta_i, \quad \delta_i \sim U(-1, 1), \quad (4)$$

where the noise term  $\alpha \delta_i$  introduces small vibrations to reduce static friction and enhance object mobility. Each actuator operates within a range of  $[-0.2, 0.2]$  m, allowing a maximum surface tilt of approximately  $\pm 38^\circ$ . Continuous updates of tilt angles and actuator positions ensure smooth, real-time manipulation.

For multi-module operation, neighboring modules share boundary actuators that are jointly controlled to form localized gradients for object transfer. This distributed approach maintains the simplicity and low-dimensionality of the single-module controller while enabling seamless, large-scale manipulation across the deformable MANTA-RAY surface.

#### IV. RESULTS

To evaluate the effectiveness of Modular MANTA-RAY system, we conducted three types of experiments on the actual hardware setup:

1. Object Passing: This experiment was conducted to determine how the relative elevation of the actuators affects the dynamic path of the object while passing the object to neighboring module, depending on its shape.

2. Object Behavior: In this experiment, various objects were passed between all modules in square trajectory on the platform. This information is crucial to identify potential extent and limitations of manipulation.

3. Target Reaching: The controller was used to move an object from its initial position to a specified goal location on the platform. This experiment was designed to evaluate the effectiveness and robustness of the controller when managing the non-linear behavior of the soft surface.

4. Multi-object Handling: Multiple objects were placed on the modules and directed to their respective target positions to check the multi-object handling capabilities of the platform.

Following subsections describe the experimental setup and results of these experiments in more details.

##### A. Object passing

During object passing, the rolling and sliding behaviors depend strongly on the object's shape and surface characteristics. The more irregular the object, the more distinct and variable its motion becomes during transfer. To ensure effective control, maintaining consistency in these behaviors is essential. To evaluate this, each object was passed from the center of the starting module (M0) to the center of an adjacent module (M2) and then back to M0. The experiment was repeated three times to assess behavioral repeatability across multiple trials.

Figure 2 presents the results of object passing for six different objects with varying shapes, sizes, friction coefficients, and weights (see Table I). The vertical lines indicate the moment when the object crosses a module boundary. Spherical objects such as the apple (Fig. 2a) and sphere (Fig. 2b) primarily exhibited consistent rolling behavior, while the disk showed similar consistency through sliding, attributed to its large contact area and low center of gravity. In contrast, the cube (Fig. 2f) and dice (Fig. 2c) displayed variations in motion across runs; the cube rolled in multiple discrete steps, whereas the dice tended to roll in single steps, reflecting differences in size and weight. The cylindrical object exhibited both rolling and sliding depending on its orientation, with greater variability when misaligned.

Quantitative analysis of trajectory consistency (Fig. 3) shows clear variation across objects. The sphere and puck exhibited the lowest mean standard deviations in all components (0.0085 m, 0.0048 m, 0.0049 m for the sphere and 0.0078 m, 0.0018 m, 0.0039 m for the puck in  $x$ ,  $y$ , and  $z$  respectively), confirming highly repeatable motion. The apple and cylinder showed slightly higher deviations, with mean standard deviations of 0.0139 m, 0.0082 m, 0.0096 m and

0.0199 m, 0.0175 m, 0.0125 m, respectively, due to mixed rolling and sliding. Irregular shapes such as the cube and dice demonstrated the largest positional variability—0.0528 m, 0.0108 m, 0.0219 m for the cube and 0.0823 m, 0.0115 m, 0.0359 m for the dice—indicating inconsistent orientation changes and reorientation during passing.

Overall, these results confirm that smoother, symmetric objects exhibit stable, repeatable trajectories, while irregular geometries and higher aspect ratios increase variability in both lateral and vertical motion. The mean positional deviation across all objects remained within 0.03 m, demonstrating consistent performance of the multi-modular MANTA-RAY during heterogeneous object transfer.

##### B. Object behavior

We investigated how the position of object transfer—whether near the center or toward the edge of the platform—affects manipulation performance. In this experiment, various objects were passed between neighboring modules along a square trajectory across the surface. Each object followed three square paths in a continuous loop of two cycles: a *normal square (blue)*, where the object passed through the center between shared actuators; a *small square (purple)*, where the transfer occurred closer to the central actuator (A4); and a *large square (yellow)*, where the object was passed farther from the central actuator (A4). Ideally, during object passing an object should move along the central path between the shared actuators, forming a perfect square trajectory as shown by the dotted red line in Fig. 4, representing the normal square. When the central actuator is raised during object passing, the object traces a larger square path, whereas raising the outer actuator between shared modules results in a smaller square path. In practice, the trajectories deviate slightly for normal squares due to the fabric's elasticity and tension distribution. Spherical objects such as the sphere and egg produced three clearly distinguishable paths corresponding to the three square sizes, while the cube primarily followed the central trajectory between shared actuators.

##### C. Target reaching

We performed a target-reaching experiment with heterogeneous objects to evaluate the precision of manipulation (see Fig. 5). Each object was placed at an initial position (green circle) and tasked to reach a target location (red star) within a threshold radius of 0.03 m (red circle). If the object's initial module differed from the target module, it was first transferred along a Manhattan path to the appropriate module. Once on the target module, the position controller was activated to achieve precise alignment within the specified boundary.

Figure 5 shows that all objects successfully reached their respective target positions within the defined threshold. Figure 6c show the target reaching in simulation for a sphere. Elongated objects, such as the egg (Fig. 5e) and the cylinder (Fig. 5f), reached the target but required small corrective zig-zag motions to fine-tune their final positions. In contrast,

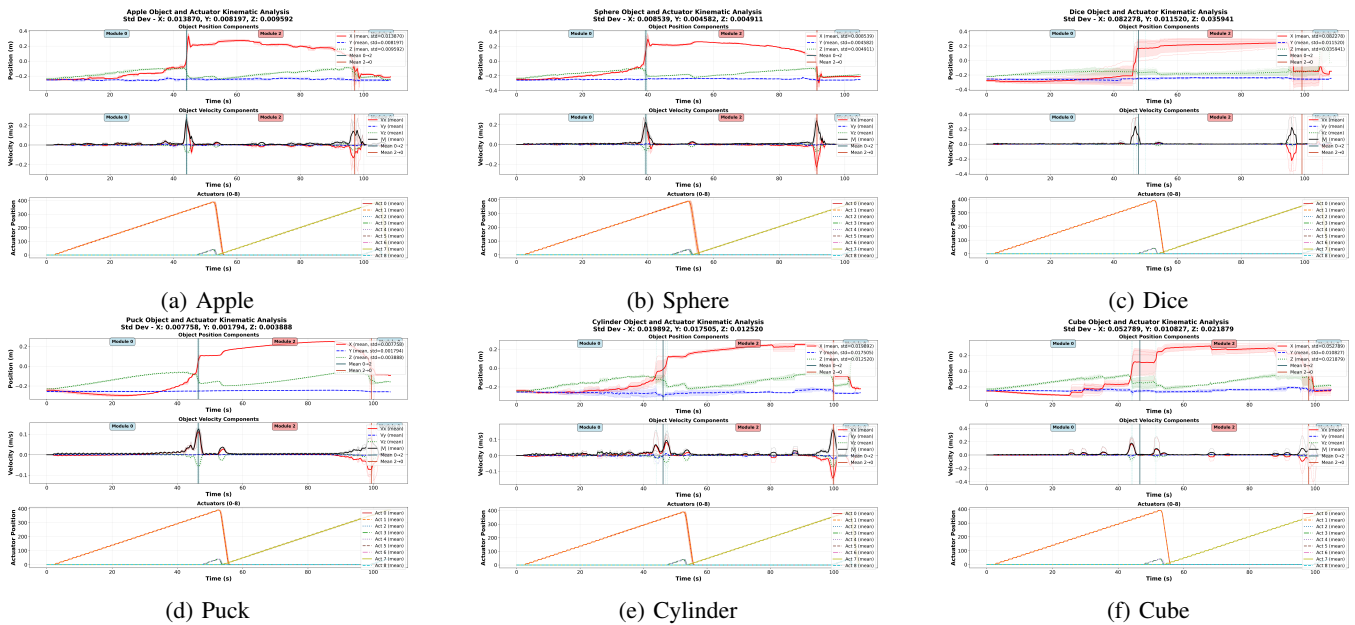


Fig. 2: Object Passing from M0 to M2 and back from M2 to M0

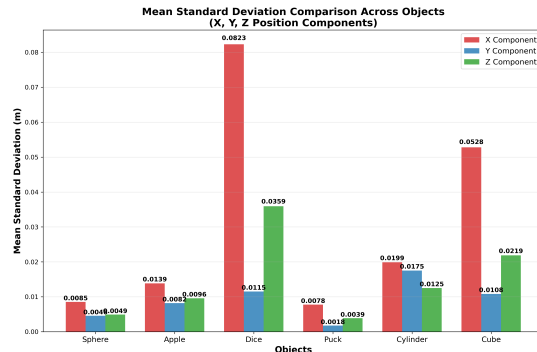


Fig. 3: Mean Standard deviation comparison across objects during passing between modules

spherical objects achieved smoother and more direct trajectories, demonstrating higher positional stability and control precision. Overall, the system achieved a mean positioning error of less than 0.02 m across all trials, confirming the controller's reliability in handling heterogeneous objects.

#### D. Multi-Object Manipulation

To evaluate the scalability and distributed coordination capability of the multi-modular MANTA-RAY, we conducted experiments involving simultaneous manipulation of two objects disk and sphere on the  $2 \times 2$  modular hardware platform. In this setup, each module operated its local controller independently, allowing parallel actuation and position control without centralized coordination. Objects were placed on different modules, a sphere on M3 and Disk on M0 and tasked to reach individual target locations M1 and M3 respectively.

Figure 6a shows the trajectories of a sphere and a disk—manipulated concurrently across separate modules.

The results demonstrate that the distributed control scheme enables stable and synchronized motion across modules. The platform maintained consistent tracking performance with an average control frequency of 20 Hz, and each object reached its target within the 0.03 m positional threshold. This confirms that the modular actuation framework can effectively support both parallel and coordinated manipulation of heterogeneous objects. We also check scalability of the platform in simulation by doing multi object target reaching on  $3 \times 3$  platform with two spherical object, see figure 6b.

Overall, these results validate the scalability of the distributed multi-module MANTA-RAY control strategy. The system is capable of performing multiple independent manipulation tasks in real time while preserving the soft, compliant nature of the deformable surface, laying the groundwork for large-scale, coordinated manipulation systems.

Object	Weight (g)	Size (cm)	Fabrication Method
Sphere	32	$\varnothing 4.5$	Molding
Cube	31	$4.2 \times 4.2 \times 4.2$	FDM 3D Printing
Disk	26	$\varnothing 7$ , Thickness: 2.5	FDM 3D Printing
Apple	120.4	$\varnothing 5-7$	—
Cylinder	71.3	$\varnothing 3$ , Height: 13	Clean Spray hand sanitizer
Egg	61.2	$\varnothing (4.1-6.2)$	—
Dice	5	$1.5 \times 1.5 \times 1.5$	Molding

TABLE I: Details of objects: weight, size, and fabrication method.

## V. DISCUSSION

The multi-modular MANTA-RAY demonstrates that soft, fabric-based manipulation can be effectively scaled using a distributed, low-dimensional control framework. The experiments confirm that simple object passing behavior combined with a linear PID controller is sufficient for robust

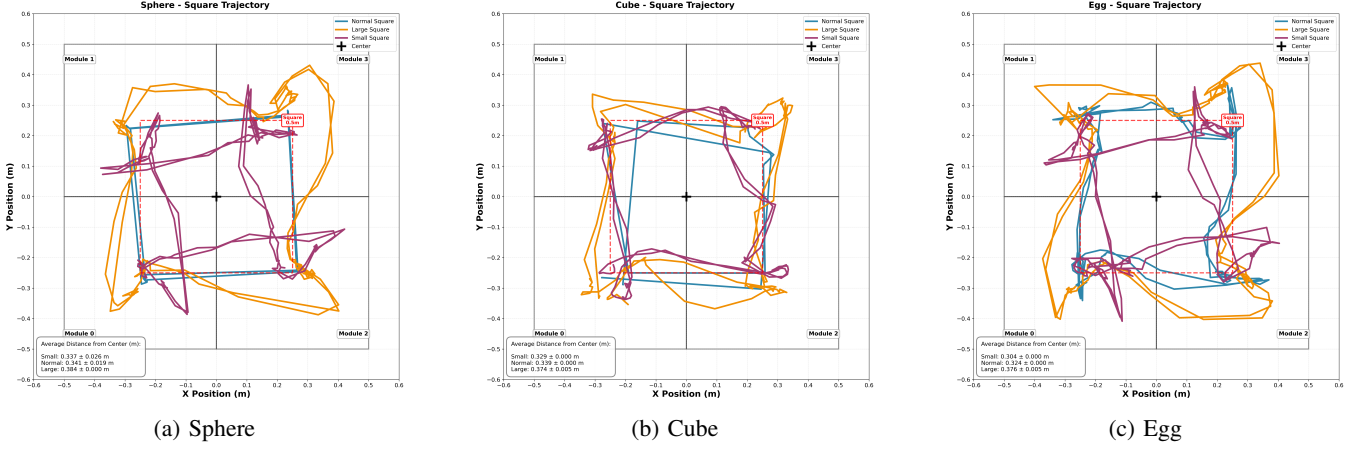


Fig. 4: Square path of the object with three paths: Normal square (Blue), Small square (Purple) and Large square (Orange)

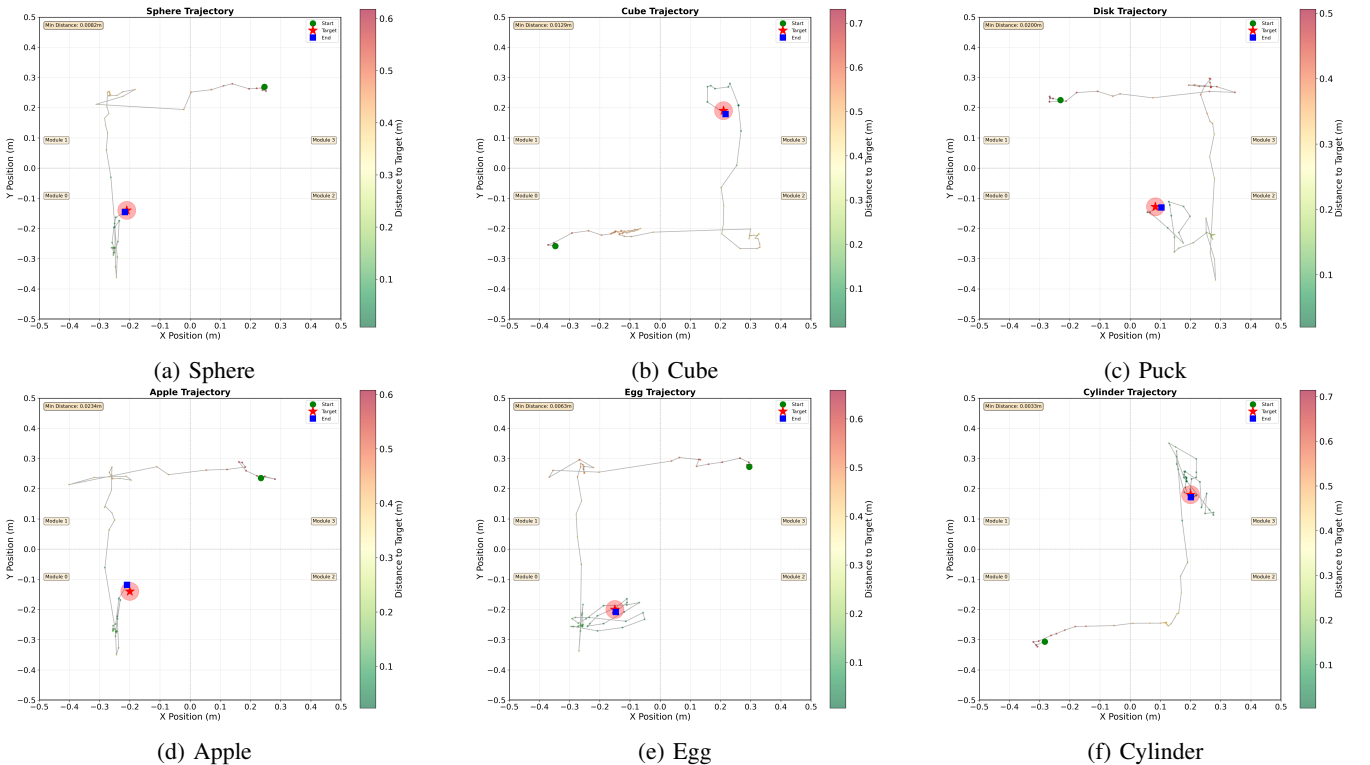


Fig. 5: Target reaching for different objects on hardware platform. Object start at initial position (green circle) and move to target location (red star) within a threshold of 3 cm (red circle) along a line path.

and repeatable manipulation of heterogeneous objects across interconnected modules. The system preserves the safety and adaptability of soft manipulation while extending its operational workspace through modular scalability.

The results show that object geometry plays a dominant role in motion behavior during inter-module transfer. Spherical and cylindrical objects exhibited consistent rolling trajectories, while flatter or irregular shapes tended to slide, with variability arising from asymmetric mass distribution and contact friction. These behavioral dependencies highlight the need for adaptive control policies that account for object-specific dynamics to improve manipulation consistency.

Object trajectories along the square paths show that most objects naturally prefer passing near the midpoint between the two shared actuators rather than following smaller or larger square paths. This behavior arises from the fabric's natural sagging between shared actuators, which forms a curved surface with the lowest point at the center, creating a gravitational bias that guides objects along this path.

Target-reaching experiments confirmed the precision of the proposed controller, achieving a positioning error below up to 1 cm for all tested objects. However, elongated or irregular objects required small corrective motions to converge to the goal, indicating that fine-grained deformation control or

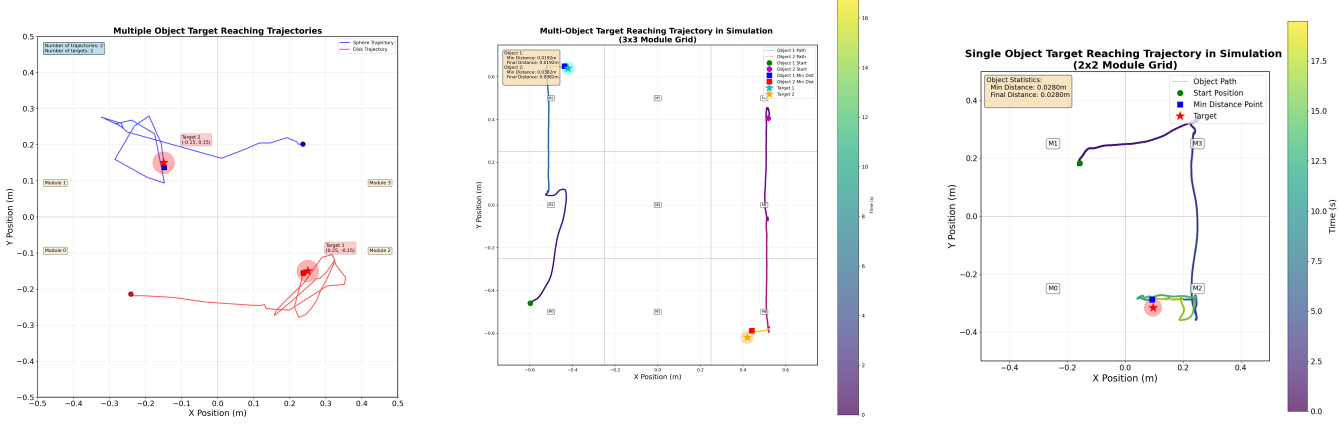


Fig. 6: Multi-object target reaching demonstrated on the MANTA-RAY platform: (a) hardware implementation, (b) simulation on a  $3 \times 3$  modular configuration. Single-object target reaching: (c) simulation on a  $2 \times 2$  platform

variable gain tuning may enhance precision. The successful demonstration of parallel manipulation highlight scalability and distributed capabilities. However parallel manipulation is limited dues to interference when adjacent modules deform simultaneously, and need for interference free controller investigation in future.

Overall, the multi-modular MANTA-RAY bridges the gap between soft, compliant manipulation and scalable surface-based robotics. Future work will focus on improving module coordination through learning-based control, integrating embedded sensing for feedback, and scaling to higher module densities to enable complex, interference free coordinated manipulation across large deformable surfaces.

## VI. CONCLUSION

This work presented the multi-modular MANTA-RAY platform, a scalable, fabric-based robotic surface capable of manipulating heterogeneous and fragile objects through distributed actuation. By integrating a simple linear PID controller with geometric transformation and an object-passing strategy, the system achieves reliable manipulation and inter-module coordination using only a low-dimensional controller. Experimental results demonstrated precise target reaching with a mean positioning error below 1 cm over the large area of  $1 \times 1$  meter with just 9 actuators and consistent object transfer across modules for diverse object types as well as parallel manipulation. Due to drastically reducing the actuator density and having a continue soft surface, this work opens the avenue to implement robotic manipulation surfaces in applications such as food processing.

## REFERENCES

- [1] Deepak Parajuli, Mark D Bedillion, and Randy C Hoover. Actuator array manipulation using low resolution local sensing. In *ASME International Mechanical Engineering Congress and Exposition*, volume 46476, page V04AT04A003. American Society of Mechanical Engineers, 2014.
- [2] Claudio Uriarte and Hendrik Thamer. Methode zur bewertung der flexibilität und wandelbarkeit am beispiel eines omnidirektionalen fördersystems. *Logistics Journal: Proceedings*, 2022(18), 2022.
- [3] Zhengrong Xue, Han Zhang, Jingwen Cheng, Zhengmao He, Yuanchen Ju, Changyi Lin, Gu Zhang, and Huazhe Xu. Arraybot: Reinforcement learning for generalizable distributed manipulation through touch. In *2024 IEEE International Conference on Robotics and Automation (ICRA)*, pages 16744–16751. IEEE, 2024.
- [4] BK Johnson, M Naris, V Sundaram, A Volchko, K Ly, SK Mitchell, E Acome, N Kellaris, C Keplinger, N Correll, et al. A multifunctional soft robotic shape display with high-speed actuation, sensing, and control. *Nature Communications*, 14(1):4516, 2023.
- [5] Ioannis Georgilas, Andrew Adamatzky, and Chris Melhuish. Cellular automaton manipulator array. *Robots and Lattice Automata*, pages 295–309, 2015.
- [6] Quan Zhou, Veikko Sariola, Kourosh Latifi, and Ville Liimatainen. Controlling the motion of multiple objects on a chladni plate. *Nature communications*, 7(1):12764, 2016.
- [7] Hyungpil Moon and Jonathan Luntz. Distributed manipulation of flat objects with two airflow sinks. *IEEE Transactions on robotics*, 22(6):1189–1201, 2006.
- [8] M Ataka, Bernard Legrand, Lionel Buchaillot, D Collard, and H Fujita. The 2d feedback conveyance with ciliary actuator arrays. In *The 13th International Conference on Solid-State Sensors, Actuators and Microsystems, 2005. Digest of Technical Papers. TRANSDUCERS’05.*, volume 1, pages 31–34. IEEE, 2005.
- [9] Satoshi Tadokoro, Satoshi Fuji, Toshi Takamori, and Keisuke Oguro. Distributed actuation devices using soft gel actuators. In *Distributed Manipulation*, pages 217–235. Springer, 2000.
- [10] Chih-Han Yu, Kristina Haller, Donald Ingber, and Radhika Nagpal. Morpho: A self-deformable modular robot inspired by cellular structure. In *2008 IEEE/RSJ International Conference on Intelligent Robots and Systems*, pages 3571–3578. IEEE, 2008.
- [11] Pratik Ingle, Kasper Støy, and Andres Faiña. Soft manipulation surface with reduced actuator density for heterogeneous object manipulation. In *2025 IEEE 8th International Conference on Soft Robotics (RoboSoft)*, pages 1–8, 2025.
- [12] Ziqiao Wang, Serhat Demirtas, Fabio Zuliani, and Jamie Paik. Surface-based manipulation, 2025.
- [13] Pratik Ingle, Kasper Støy, and Andres Faiña. Heterogeneous object manipulation on nonlinear soft surface through linear controller. In *2025 IEEE 21st International Conference on Automation Science and Engineering (CASE)*, pages 1780–1787, 2025.
- [14] Emanuel Todorov, Tom Erez, and Yuval Tassa. Mujoco: A physics engine for model-based control. In *2012 IEEE/RSJ International Conference on Intelligent Robots and Systems*, pages 5026–5033. IEEE, 2012.